PROTEINS: Structure, Function, and Genetics 14:363–371 (1992)

Crystal Structure of Human Immunoglobulin Fragment Fab New Refined at 2.0 Å Resolution

Frederick A. Saul and Roberto J. Poljak
Département d'Immunologie, Institut Pasteur, 75724 Paris Cedex 15, France

ABSTRACT **The three-dimensional structure of the human immunoglobulin fragment Fab New (IgG1, λ) has been refined to a crystallographic *R*-factor of 16.9% to 2 Å resolution. Rms deviations of the final model from ideal geometry are 0.014 Å for bond distances and 3.03° for bond angles. Refinement was based on a new X-ray data set including 28,301 reflections with $F>2.5\sigma(F)$ from 6.0 to 2.0 Å resolution. The starting model for the refinement procedure reported here is from the Brookhaven Protein Data Bank entry 3FAB (rev. 1981). Differences between the initial and final models include modified polypeptide-chain folding in the third complementarity-determining region (CDR3) and the third framework region (FR3) of V_H and in some exposed loops of C_L and C_H1. Amino acid sequence changes were determined at a number of positions by inspection of difference electron density maps. The incorporation of amino acid sequence changes results in an improved V_H framework model for the "humanization" of monoclonal antibodies.**

Key words: human myeloma protein, X-ray crystallography, molecular dynamics, humanized antibodies

INTRODUCTION

The three-dimensional structure of the human myeloma immunoglobulin fragment Fab New (IgG1, λ), reported previously,[1–3] has provided novel information about the quaternary structure of antibodies, the polypeptide chain folding of the variable (V_L, V_H) and constant (C_L, C_H1) domains, and the structural role of the complementarity-determining regions (see review, ref. 4). We report here the crystallographic refinement of Fab New based on a more complete data set to 2 Å resolution obtained by the use of an X-ray area detector.

The starting model for the refinement procedure described here was taken from the Brookhaven Protein Data Bank[5] entry 3FAB (1981). This structure had been refined to a nominal resolution of 2 Å with a limited X-ray data set including approximately 12,000 reflections measured from 12 crystals by means of a four-circle diffractometer.[2,3] The starting model from the Protein Data Bank included a number of amino acid sequence changes based on chemical sequencing data and had been refined (Amzel, Saul, and Poljak, unpublished) with the program PROLSQ[6] subsequent to the previously reported refinement procedure.

The three-dimensional structure of Fab New described here exhibits better overall stereochemistry compared with the previous model and includes a number of changes in polypeptide-chain conformation, particularly in the third complementarity-determining region (CDR3) and in the third framework region (FR3) of V_H, and in several exposed loops of C_L and C_H1 (see ref. 7 for the definition of CDR and FR regions; also see Fig. 1). The model includes amino acid sequence modifications in V_L, V_H, and C_L determined during the refinement process by inspection of electron density maps.

MATERIALS AND METHODS

X-Ray Data Collection

Crystals of Fab New belong to space group $C2$ ($a=111.43$ Å, $b=56.68$ Å, $c=90.30$ Å, $\beta=116.46°$) with one Fab molecule in the asymmetric unit.[1] X-Ray data were measured from two crystals of approximate dimensions 0.16 × 0.5 × 0.6 mm and 0.12 × 0.3 × 0.6 mm, respectively, from the same crystallization batch used in the previous structural studies of Fab New.[1–3]

X-ray intensities were measured with a Nicolet/Siemens (Xentronics) area detector using CuK_α radiation from a Rigaku RU200 rotating anode generator equipped with a graphite monochromator. Detector image frames were measured using an ω-scan step size of 0.2° with a crystal-detector distance of 120 mm and a detector 2θ angle of 28°. The exposure time was 300 sec per frame. Total ω rotation was 180° and 200°, respectively, for 2 orientations of the larger crystal. Additional data from 60° rotation of the smaller crystal was included in the final merged data set to provide increased coverage of reciprocal space at high resolution.

Received November 19, 1991; revision accepted February 14, 1992.

Address reprint requests to Frederick Saul, Département d'Immunologie, Institut Pasteur, 25, rue du Docteur Roux, 75724 Paris Cedex, France.

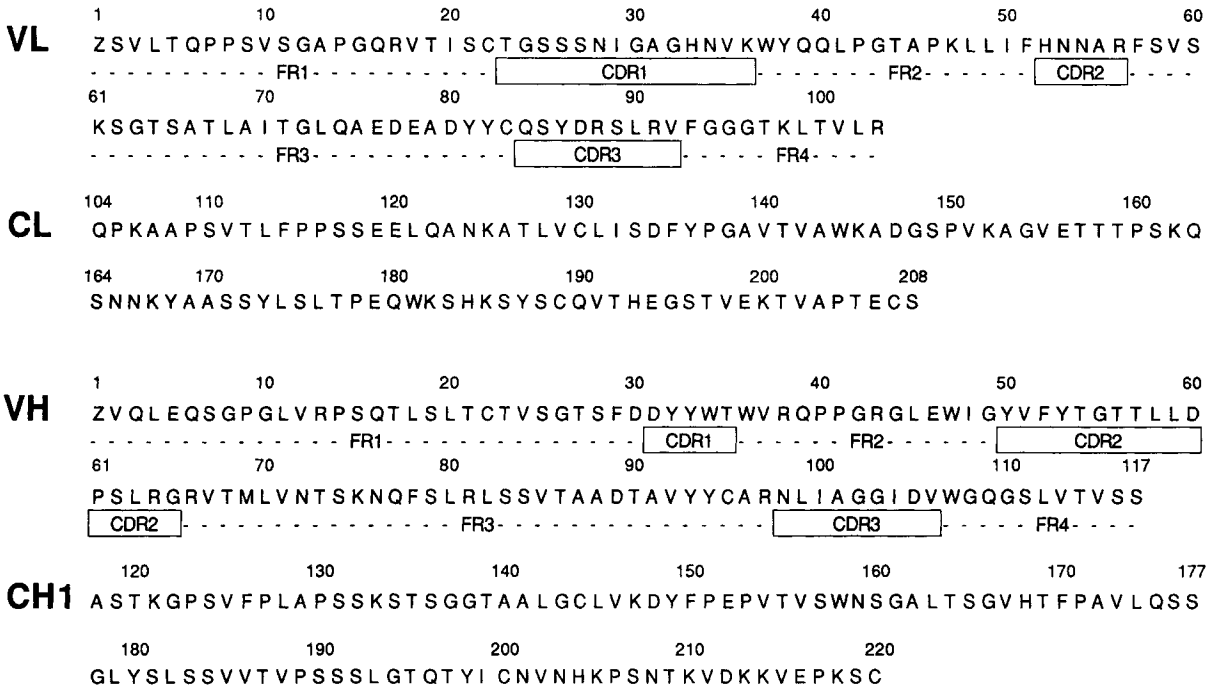

Fig. 1. Amino-acid sequence of Fab New. Z: pca, pyrrolidone carboxylic acid. The CDRs and framework (FR) regions (as defined by Kabat et al.[7]) of V_L and V_H are indicated. Residues are numbered sequentially within each polypeptide chain; residue numbers do not necessarily correspond to those of refs. 1, 2, 3, or 7. Note: compared with other human λ chains[7] a deletion of seven residues occurs between positions 56 and 57 (Kabat positions 54 and 62) in V_L New. Modifications to the previously reported[3] sequence of V_H were determined by protein sequencing techniques (Chiu and Poljak, unpublished); these changes were included in the previous structure of Fab New submitted to the Brookhaven Protein Data Bank (1981). Additional sequence changes were determined in V_H, V_L, and C_L by inspection of difference electron density maps during the course of the refinement procedure described here (see text).

The data were processed and X-ray intensities obtained with the program system XDS.[8] Integrated intensities were scaled in batches of 5° rotation and merged using the programs ROTAVATA and AGROVATA[9] of the CCP4-Daresbury program package.[10] Structure factors were modified to follow Wilson's distribution[11] by the method of French and Wilson[12] using the program TRUNCATE of the CCP4 package. The overall value of R_{merge} on intensities was 7.9% for 28,429 unique reflections determined from 80,611 measurements in the resolution range of 6.0 to 2.0 Å (see summary of data statistics, Table I); 28,301 reflections for which $F>2.5\sigma(F)$ from 6.0 to 2.0 Å were included in the crystallographic refinement procedure.

Crystallographic Refinement

Refinement of atomic coordinates was carried out by simulated annealing (SA) with the program X-PLOR.[13] Seventeen cycles of SA refinement were performed at a heatstage temperature of 2,000 K in 0.001 psec steps with 500 or 1,000 heatstage steps per cycle, using ideal structure factor amplitude weights (W_A) as determined by X-PLOR. Individual restrained isotropic temperature factors were refined after each cycle with target values of 1.5σ for main-chain atoms and 2.0σ for side chains. Four final cycles of refinement were carried out at a heatstage temperature of 1,000 K with slow cooling[14] from 1,000 K to 300 K in 50 K steps. Calculations were performed on a Convex C210 computer.

Main chain ϕ,ψ angles and deviations of bond distances and angles from ideal values were monitored after each cycle of refinement. Manual corrections were made to the model by inspection of $2F_o-F_c$ and F_o-F_c electron density maps displayed on an Evans and Sutherland PS390 graphics system using the program FRODO.[15] The structures of human Fab fragments Kol[16] (Brookhaven Protein Data Bank entry 2FB4) and Hil (Saul and Poljak, refinement in progress), as well as those of other Fab structures available from the Brookhaven Protein Data Bank, were compared with the model during the rebuilding process to indicate possible corrections in areas of poor stereochemistry or weak electron density. Solvent (water) molecules, initially excluded from the model, were added during the latter stages of refinement by a search procedure based on peaks in difference maps and bond-distance criteria. Proposed water molecules were verified after refinement by inspection of electron density maps. Solvent occupancies were not refined. Water molecules for

TABLE I. Data Statistics*

Resolution range (Å)	Number of reflections merged	Number of unique merged reflections	R_{merge}†	Average $I/\sigma(I)$
6.00–4.47	5053	1630	0.050	11.7
4.47–3.72	6713	2110	0.054	11.3
3.72–3.25	8086	2518	0.061	10.5
3.25–2.93	8806	2846	0.076	9.2
2.93–2.68	9091	3076	0.106	7.0
2.68–2.49	9115	3197	0.149	5.1
2.49–2.34	8938	3298	0.190	4.0
2.34–2.21	8913	3381	0.230	3.2
2.21–2.10	8487	3344	0.298	2.5
2.10–2.00	7409	3029	0.400	1.8
6.00–2.00	80611	28429	0.079	

*31,779 unique reflections (93% of total possible number) were obtained in the range of 6.0 to 2.0 Å; 3,519 measurements were eliminated by various rejection criteria during merging of the data with the program AGROVATA.[10]

†$R_{merge} = \sum_{hkl}\sum_n|\langle I\rangle - I_n|/\sum_{hkl}\sum_n I_n$.

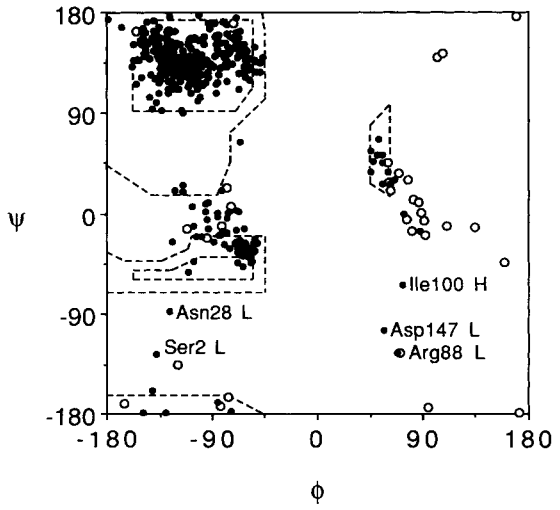

Fig. 2. Ramachandran plot of main-chain dihedral angles of Fab New. The regions of acceptable van der Waals contacts are indicated. Open circles denote glycines. Residues outside of accepted regions include Ser-2, Asn-28, Arg-88, and Asp-147 of the light (L) chain, and Ile-100 of the heavy (H) chain (see text).

which B-values exceeded 80 Å^2 after refinement were rejected.

RESULTS AND DISCUSSION

Refinement Results

The final crystallographic R factor is 16.9% for 28,301 reflections with $F>2.5\sigma(F)$ (83% of the total possible number) from 6.0 to 2.0 Å resolution. The R factor is 17.9% for all measured reflections (93% of total) from 6.0 to 2.0 Å. The distribution of R-values and number and percentage of reflections as a function of resolution are shown in Table II. Rms deviations of the structure from ideal geometry are 0.014 Å for bond distances and 3.03° for bond angles as determined by X-PLOR. The model of Fab New includes 413 amino acid residues and 229 solvent (water) molecules. *Cis*-Proline residues occur at position 137 of C_L and positions 151 and 153 of C_H1 (residue numbering refers to Fig. 1).

TABLE II. Distribution of *R*-Values After Refinement

Resolution range (Å)	Number of reflections, $F>2.5\sigma(F)$	Total possible number of reflections (%)	R*
6.00–3.70	3715	86	0.118
3.70–3.07	4101	97	0.140
3.07–2.72	3938	92	0.177
2.72–2.49	3724	87	0.201
2.49–2.32	3585	83	0.225
2.32–2.19	3405	80	0.222
2.19–2.09	3118	77	0.242
2.09–2.00	2715	63	0.268
6.00–2.00	28301	83	0.169

*$R = \sum|Fobs-Fcalc|/\sum|Fobs|$.

The distribution of main-chain dihedral angles indicates acceptable overall main-chain geometry for most residues as shown by the Ramachandran plot[17] in Figure 2. Exceptions include Ser-2, Asn-28, Arg-88, and Asp-147 of the light chain, and Ile-100 of the heavy chain (see description of structure, below). Evaluation of the intrinsic accuracy of atomic coordinates by the method of Luzzati[18] indicates a mean overall error of 0.25 Å. The average atomic temperature factor is 29 Å^2 for main-chain atoms, 32 Å^2 for side chains, and 49 Å^2 for solvent molecules. The variation of the average atomic temperature factor as a function of residue number in the light (L) and heavy (H) chains is shown in Figure 3. Relatively high temperature factors occur in several solvent-exposed loops on the surface of the molecule, particularly in C_L and C_H1.

$2F_o-F_c$ electron density maps contoured at the 1σ level show good resolution and continuity of density, with a few exceptions. A major break in main-chain density occurs between residues 131 and 138 of C_H1 in an external loop; these residues are probably disordered in the crystal structure and have been omitted from the final model. The C-terminal residues 218 to 220 of C_H1 and 205 to 208 of C_L (including the interchain disulfide bond) also lack continuous density and have been omitted from the model. Weak electron density is seen at residues 190 to 195 of C_H1 with some gaps in density for the main chain in this region. The side chains of several exposed residues (including Glu-76, Arg-88 of V_L, Lys-152, Asn-166, Glu-179, Lys-182 of C_L, Gln-3, Asp-31, Gln-109 of

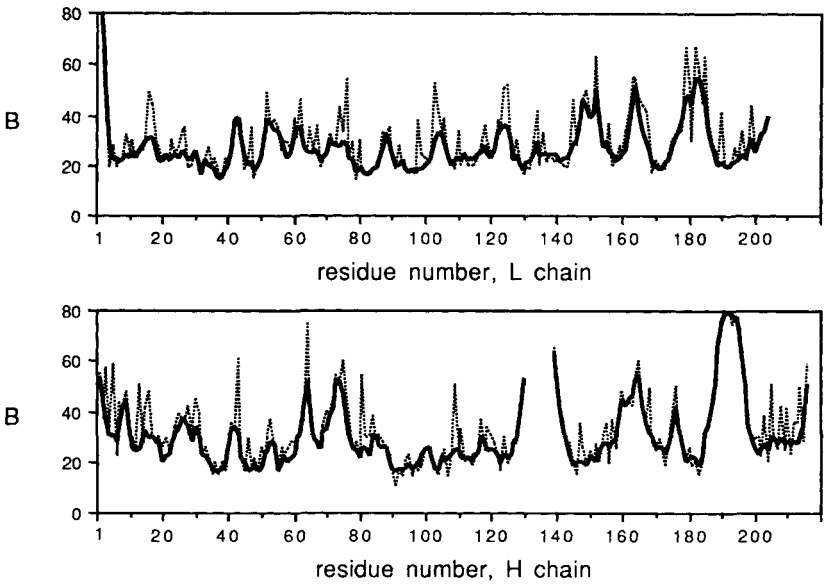

Fig. 3. Variation of the average atomic temperature factor (B, Å^2) along the light (L) and heavy (H) polypeptide chains. Solid lines represent the average B-values of main-chain atoms; broken lines represent the average B-values of side chains. The break from 131 to 138 in the H chain corresponds to uninterpreted residues which have been omitted from the final model.

V_H, and Ser-165 of C_H1) lack continuous density at the 1σ contour level, or in some cases show evidence of multiple conformation (see below). No attempt was made to refine multiple conformations of the main chain or of side chains.

The following amino acid sequence changes were determined in V_H based on $2F_o-F_c$ electron density maps (previous assignments are shown in parentheses): Trp-34 (Ser) in CDR1, Thr-54 (His), Thr-57 (Ser), Leu-58 (Asp), Leu-59 (Thr), Pro-61 (Thr), Ser-62 (Pro) in CDR2, and Gly-103 (Cys) in CDR3. (Note: V_H residue 103 is equivalent to position 100 in the sequence numbering of Kabat et al.[7]) Sequence changes were also introduced at V_L residues His-33 (Asn) and Asn-34 (His) in CDR1, and Thr-64 (Ser) in FR3 (Kabat positions 31, 32, and 69, respectively). These modifications are included in the amino acid sequence shown in Figure 1. The determination of sequence modifications based on electron density maps is unambiguous in most cases. The assignments of Trp-34, Thr-57, Pro-61, and Ser-62 of V_H correspond to the most frequently occurring residues at these positions in human V_H subgroup II.[7] Similarly, Thr-64 of V_L (Kabat position 69) is the most frequently occurring residue at this position in sequences of human λ-chain subgroup I.[7] The occurrence of Trp at V_H position 34 is clearly indicated by the electron density (Fig. 4). This assignment is not inconsistent with the chemical sequencing data, as the presence of Trp had been analyzed qualitatively and a Trp residue also occurs at position 36, whereas Ser is frequently assumed to occur at a position giving no amino acid signal in later cycles of Edman degradation. Some uncertainties remain, however, including Leu-59 of V_H which could be interpreted as Asp or Asn based on possible hydrogen bonding to a nearby side chain and water molecule, and Arg-88 in CDR3 of V_L, for which no significant side-chain density is seen. The absence of electron density for the side chain of V_L residue 88 may be due to multiple conformation or disorder of the Arg side chain;

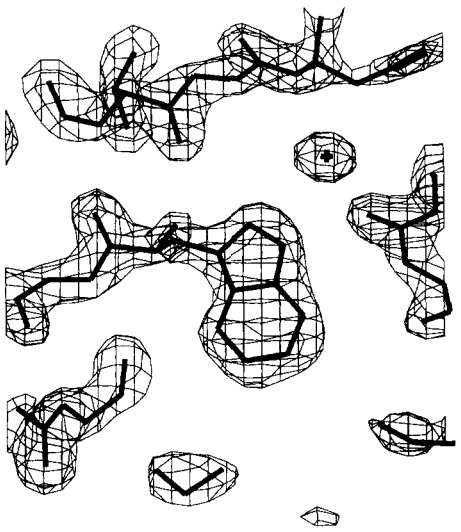

Fig. 4. View of V_H residue Trp-34 (center) and surrounding residues, superimposed on the corresponding $2F_o-F_c$,αc electron density map contoured at 2σ. Residue 34 was changed from Ser in the previous model of Fab New (see text).

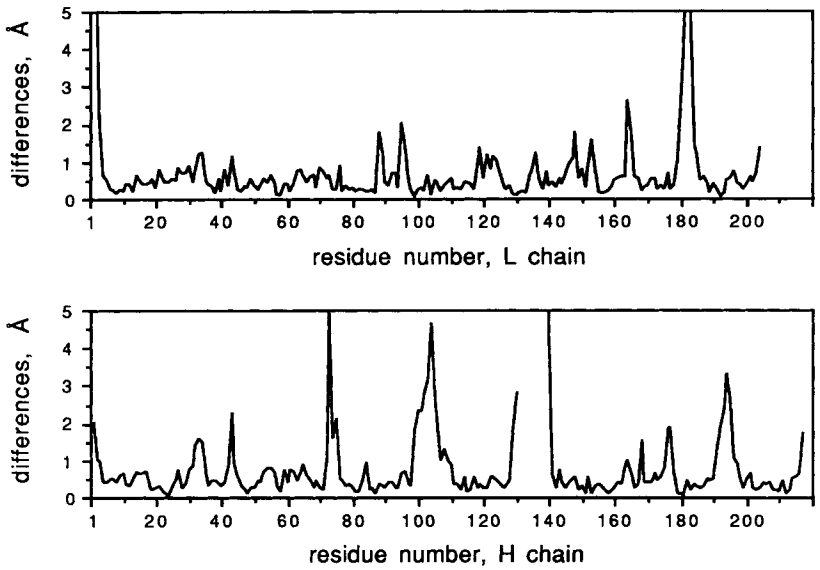

Fig. 5. Rms differences between α-carbon positions of the initial and final models of Fab New (L: light chain, H: heavy chain).

this residue exhibited main-chain dihedral angles outside the accepted regions ($\phi = 68°$, $\psi = -124°$, see Fig. 2) and was refined as Gly during the final stages of the crystallographic refinement procedure.

An additional sequence change was introduced at Gly-148 (Ser) in C_L. Residue 148 (Kabat position 152) occurs at a bend in the polypeptide chain which involves unfavorable main-chain dihedral angles at Asp-147 ($\phi = 57°$, $\psi = -104°$), and some uncertainty remains as to the correct interpretation of the electron density for this loop.

Description of Structure and Comparison With the Starting Model

The overall quaternary structure of Fab New and the predominant β-sheet folding of the polypeptide chain (the immunoglobulin fold) within V_L, V_H, C_L, and C_H1 have been described.[1-3] The hydrogen-bonding patterns within the β-sheets are as reported previously, although significant changes in conformation are seen in several loops (including CDR3 and a loop in FR3 of V_H) on comparing the initial and final models (see Figs. 5 and 6). A stereo view of the CDRs at the antigen-combining site is shown in Figure 7. The combining site cavity contains a number of water molecules which form a network of hydrogen bonds with CDR and framework residues. In particular, a deeply buried water molecule (temperature factor: 21.6 Å^2) forms hydrogen bonds with Thr-35, Trp-47, and Asn-98 of V_H (in CDR1, FR2, and CDR3, respectively) which could play an important role in the stabilization of interactions between the three V_H CDR segments.

The greatest differences in conformation between the initial and final models occur at residues 1–3, 164–165, and 180–184 of the light chain, and at residues 72–75 (in FR3), 98–105 (CDR3), 131 and 140, and 191–195 of the heavy chain (see Figs. 5 and 6). N-Terminal residues 1–3 of V_L show evidence of multiple conformation (see below), and V_H residues 98–105 in CDR3 include a sequence change at Gly-103 (changed from Cys in the previous model). In the final structure, residues 164, 165, and 180–184 of the light chain, and 72–75 and 191–195 of the heavy chain have similar conformations to those of the equivalent residues in human Fabs Kol[16] and Hil (Saul and Poljak, unpublished results). Other differences between the initial and final models include the partial rotation of peptide bonds at residues 33, 94, 95, 151 in the light chain, and 1, 43, 84, 165, 176, 178, and 189 in the heavy chain.

The structure has main-chain dihedral angles outside accepted regions at Asn-28 in CDR1 of V_L (Kabat position 27B; $\phi = -126°$, $\psi = -88°$, see Fig. 2) and Ile-100 in CDR3 of V_H (Kabat position 97; $\phi = 73°$, $\psi = -64°$) although the electron density is well defined and appears to confirm the conformation of the main chain and side chains at these positions. Relatively weak density and high atomic temperature factors occur at the N-terminal residues 1 to 3 of V_L, with unfavorable main-chain dihedral angles at Ser-2 ($\phi = -138°$, $\psi = -126°$). These N-terminal residues are exposed to solvent near CDR1 and CDR3 of V_L. The electron density suggests two possible paths for the main chain at V_L residues 1 and 2.

Extensive intermolecular contacts are made by residues of C_H1 about a crystallographic 2-fold axis at (0,y,1/2), forming a six-stranded antiparallel β sheet structure between two symmetry-related mol-

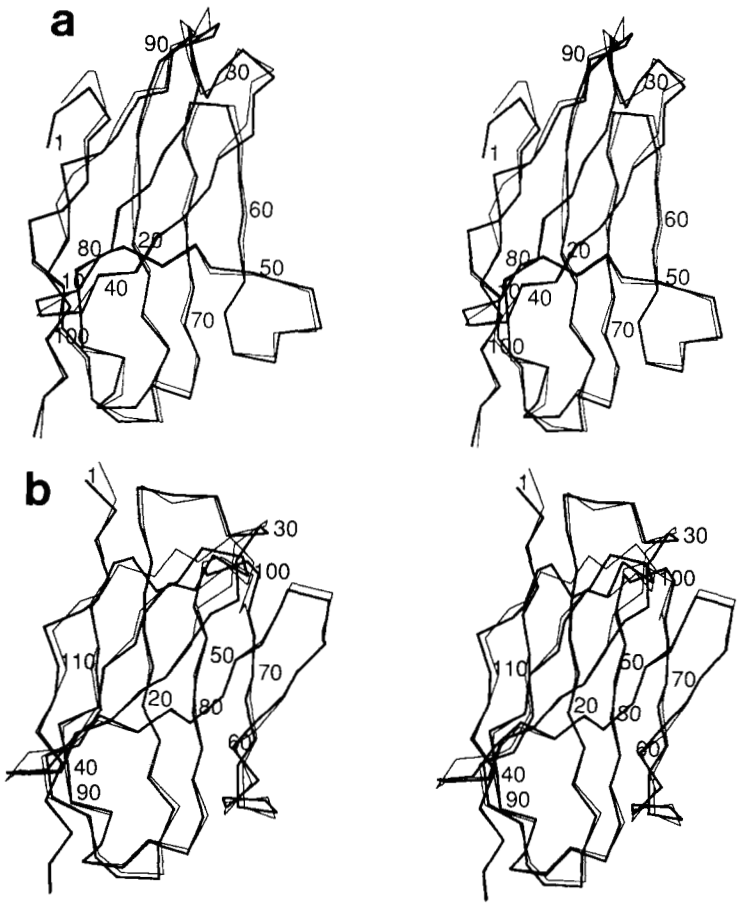

Fig. 6. Comparison of α-carbon positions of the initial model (thin lines) and final model (thick lines) of Fab New (**a:** V_L, **b:** V_H, **c:** C_L, **d:** C_H1). Residues 131 to 138 and 218 to 220 of C_H1 and 205 to 208 of C_L are not included in the final model (see text). Parts c and d appear on facing page.

ecules (Fig. 8). Many side chains and water molecules are involved in intermolecular contacts in this region, including a water molecule (not added to the model) located on the 2-fold axis. This feature of crystal packing involves residues that are highly conserved in C_H1 sequences. A six-stranded β sheet structure formed across a 2-fold axis has also been reported[19,20] in the C_L domains in crystals of the Bence–Jones proteins Mcg[19] and Loc.[20]

V_H Framework Model

Procedures to "humanize" murine monoclonal antibodies by inserting mouse CDRs onto human framework structures (see review, ref. 21) and proposals to substitute certain surface framework residues of murine antibodies with the corresponding human framework residues[22] have led to increased interest in models of human Fab structures. Reshaped human–murine antibodies used in human therapy trials have been shown to be less immunogenic than mouse antibodies while retaining desired antigen-binding specificity.[23,24]

The V_H region of Fab New has been used as a framework model for the insertion of specific CDRs[25–27] in efforts to humanize murine antibodies. In some of these studies Ser-27 in FR1 of the engineered human–murine chimeric antibodies was changed to Phe in order to restore hydrophobic packing interactions in the loop region extending from residue 27 to 34. (An aromatic residue, Phe or Tyr, occurs at position 27 in some other human and mouse H chains.) In the structure of Fab New, V_H position 27 is occupied by Thr, which would not be expected to maintain the same packing of this loop. However, hydrophobic packing is maintained by Trp-34 in the structure of V_H New (see Fig. 9), changed from Ser in the previous model. This structural motif may also apply to mouse V_H sequences of subgroup IA, in which position 27 is frequently occupied by Asp and position 34 by Trp (see ref. 7 for the classification of variable region subgroups).

The sequence of the V_H framework of Fab New (human subgroup II) differs in several segments from those of the human Fabs Kol and Hil (subgroup III) and from some mouse V_H sequences, although V_H New appears to be more closely homologous to

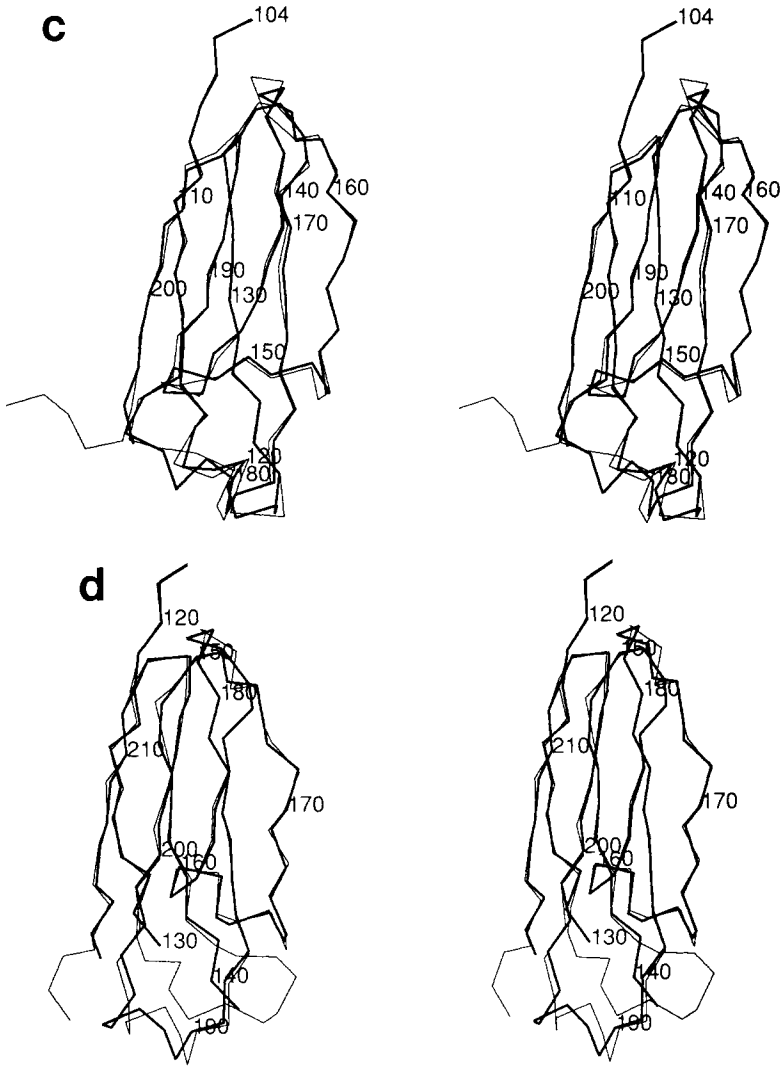

Fig. 6c,d. Parts a and b and legend appear on previous page.

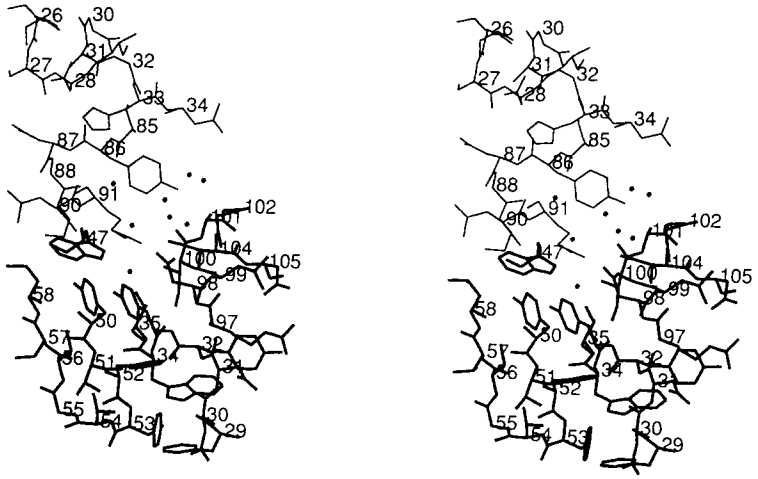

Fig. 7. Stereo view of the complementarity-determining regions (CDRs) and some framework (FR) residues of Fab New (thin lines, upper left: V_L; thick lines, lower right: V_H). Significant differences occur in the conformation of CDR3 of V_H, compared with the previous model (see text). Several water molecules (indicated) occupy the combining-site cavity (see text). Residue numbering refers to Figure 1.

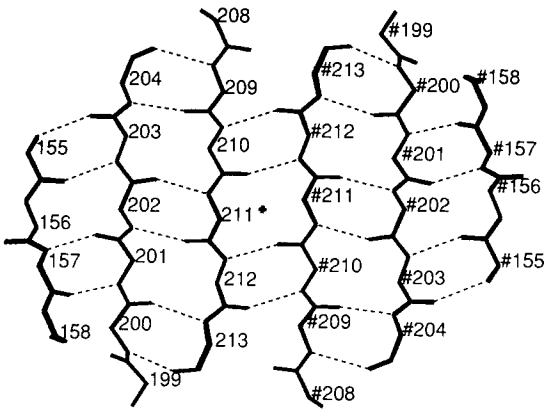

Fig. 8. Main-chain atoms of the C_H1 regions of two symmetry-related molecules which form a six-stranded antiparallel β-sheet structure about a crystallographic 2-fold axis (see text). Residue numbers preceeded by the symbol # on the right of the figure are related by the 2-fold axis to equivalent residues on the left. Residue numbering refers to Figure 1. The 2-fold axis (indicated, center) is perpendicular to the plane of the figure. Hydrogen bonds are indicated by broken lines.

mouse sequences such as those of subgroup IA. Fab New may therefore provide a better V_H framework model for the insertion of CDRs derived from some monoclonal antibodies of murine origin.

Atomic coordinates have been deposited with the Brookhaven Protein Data Bank, entry 7FAB.

ACKNOWLEDGMENTS

This work was supported by grants from the CNRS, Institut Pasteur, and the Fondation Louis Jeantet.

REFERENCES

1. Poljak, R.J., Amzel, L.M., Avey, H.P., Chen, B.L., Phizackerley, R.P., Saul, F. Three-dimensional structure of the Fab' fragment of a human immunoglobulin at 2.8-Å resolution. Proc. Natl. Acad. Sci. U.S.A. 70:3305–3310, 1973.
2. Poljak, R.J., Amzel, L.M., Chen, B.L., Phizackerley, R.P., Saul, F. The three-dimensional structure of the Fab' fragment of a human myeloma immunoglobulin at 2.0-Å resolution. Proc. Natl. Acad. Sci. U.S.A. 71:3440–3444, 1974.
3. Saul, F.A., Amzel, L.M., Poljak, R.J. Preliminary refinement and structural analysis of the Fab fragment from human immunoglobulin New at 2.0 Å resolution. J. Biol. Chem. 253:585–597, 1978.
4. Amzel, L.M., Poljak, R.J. Three-dimensional structure of immunoglobulins. Annu. Rev. Biochem. 48:961–997, 1979.
5. Bernstein, F.C., Koetzle, T.F., Williams, G.J.B., Meyer, E.F., Jr., Brice, M.D., Rodgers, J.R., Kennard, O., Shimanouchi, T., Tasumi, M. The Protein Data Bank: A computer-based archival file for macromolecular structures. J. Mol. Biol. 112:535–542, 1977.
6. Hendrickson, W.A., Konnert, J. In: "Biomolecular Structure, Function, Conformation and Evolution," Vol. 1. Srinivasan, R. (ed.). New York: Pergamon Press, 1981: 43–47.
7. Kabat, E.A., Wu, T.T., M., Perry, H.M., Gottesman, K.S., Foeller, C. "Sequences of Proteins of Immunological Interest," 5th ed. U.S. Department of Health and Human Services, 1991.
8. Kabsch, W. Evaluation of single-crystal X-ray diffraction data from a position-sensitive detector. J. Appl. Crystallogr. 21:916–924, 1988.
9. Fox, G.C., Holmes, K.C. An alternative method of solving the layer scaling equations of Hamilton, Rollet and Sparks. Acta Crystallogr. 20:886–891, 1966.
10. CCP4, 1979. The SERC (UK) Collaborative Computing Project No. 4, a suite of programs for protein crystallography. Distributed from Daresbury Laboratory, Warrington, WA4 4AD, UK.
11. Wilson, A.J.C. The probability distribution of X-ray intensities. Acta Crystallogr. 2:318–321, 1949.
12. French, S., Wilson, K. On the treatment of negative intensity observations. Acta Crystallogr. A34:517–525, 1978.
13. Brünger, A.T., Kuriyan, J., Karplus, M. Crystallographic *R* factor refinement by molecular dynamics. Science 235: 458–460, 1987.
14. Brünger, A.T., Krukowski, A. Slow-cooling protocols for crystallographic refinement by simulated annealing. Acta Crystallogr. A46:585–593, 1990.

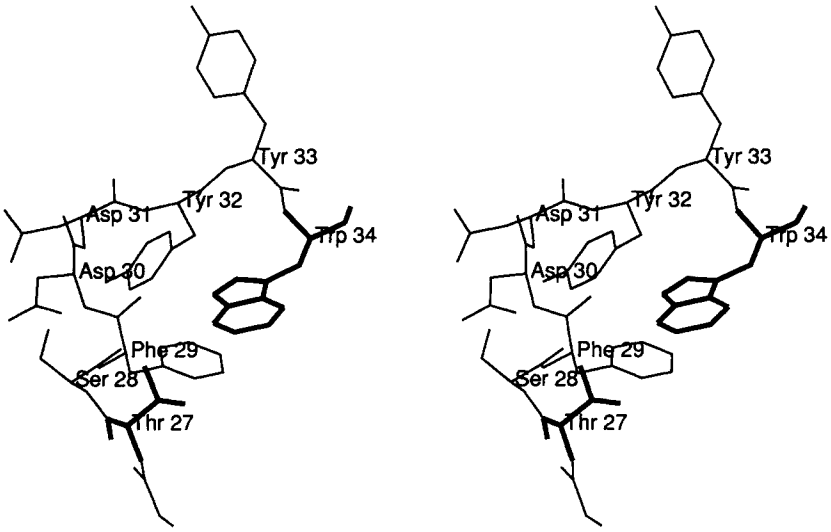

Fig. 9. Stereo view of residues in a loop between Thr 27 and Trp 34 of V_H. Trp 34 was changed from Ser in the previous model of Fab New. Position 27 is occupied by an aromatic residue (Phe or Tyr) in some other Fab structures (see text). Residues Trp 34 and Thr 27 of Fab New are indicated by thick lines.

15. Jones, A. A graphics model building and refinement system for macromolecules. J. Appl. Crystallogr. 11:268–272, 1978.
16. Marquart, M., Deisenhofer, J., Huber, R., Palm, W. Crystallographic refinement and atomic models of the intact immunoglobulin molecule Kol and its antigen-binding fragment at 3.0Å and 1.9Å resolution. J. Mol. Biol. 141: 369–391, 1980.
17. Ramachandran, G.N., Sasisekharan, V. Conformation of polypeptides and proteins. Adv. Protein Chem. 23:283–437, 1968.
18. Luzzati, V. Traitement statistique des erreurs dans la détermination des structures cristallines. (1952). Acta Crystallogr. 5:802–810, 1952.
19. Ely, K.R., Firca, J.R., Williams, K.J., Abola, E.E., Fenton, J.M., Schiffer, M., Panagiotopoulos, N.C., Edmundson, A.B. Crystal properties as indicators of conformational changes during ligand binding or interconversion of Mcg light chain isomers. Biochemistry 17:158–167, 1978.
20. Chang, C.-H., Short, M.T., Westholm, F.A., Stevens, F.J., Wang, B.-C., Furey, W., Jr., Solomon, A., Schiffer, M. Novel arrangement of immunoglobulin variable domains: X-ray crystallographic analysis of the λ-chain dimer Bence-Jones protein Loc. Biochemistry. 24:4890–4897, 1985.
21. Winter, G., Milstein, C. Man-made antibodies. Nature (London) 349:293–299, 1991.
22. Padlan, E.A. A possible procedure for reducing the immunogenicity of antibody variable domains while preserving their ligand-binding properties. Mol. Immunol. 28: 489–498, 1991.
23. Queen, C., Schneider, W.P., Selick, H.E., Payne, P.W., Landolfi, N.F., Duncan, J.F., Avdalovic, N.M., Levitt, M., Junghans, R.P., Waldmann, T.A. A humanized antibody that binds to the interleukin 2 receptor. Proc. Natl. Acad. Sci. U.S.A. 86:10029–10033, 1989.
24. Gorman, S.D., Clark, M.R., Routledge, E.G., Cobbold, S.P., Waldmann, H. Reshaping a therapeutic CD4 antibody. Proc. Natl. Acad. Sci. U.S.A. 88:4181–4185, 1991.
25. Jones, P.T., Dear, P.H., Foote, J., Neuberger, M.S., Winter, G. Replacing the complementarity-determining regions in a human antibody with those from a mouse. Nature (London) 321:522–525, 1986.
26. Riechmann, L., Clark, M., Waldmann, H., Winter, G. Reshaping human antibodies for therapy. Nature (London) 332:323–327, 1988.
27. Verhoeyen, M., Milstein, C., Winter, G. Reshaping human antibodies: Grafting an antilysozyme activity. Science 239: 1534–1536, 1988.